

UC Irvine

UC Irvine Previously Published Works

Title

Structure-Based Simulation and Sampling of Transcription Factor Protein Movements along DNA from Atomic-Scale Stepping to Coarse-Grained Diffusion.

Permalink

<https://escholarship.org/uc/item/9s7562qt>

Journal

Journal of Visualized Experiments, 2022(181)

ISSN

1940-087X

Authors

E, Chao
Dai, Liqiang
Tian, Jiaqi
[et al.](#)

Publication Date

2022

DOI

10.3791/63406

Peer reviewed

Structure-Based Simulation and Sampling of Transcription Factor Protein Movements along DNA from Atomic-Scale Stepping to Coarse-Grained Diffusion

Chao E^{*1}, Liqiang Dai^{*1,2}, Jiaqi Tian^{3,4}, Lin-Tai Da⁴, Jin Yu^{5,6,7}

¹ Beijing Computational Science Research Center ² Shenzhen JL Computational Science and Applied Research Institute ³ School of Medical Informatics and Engineering, Xuzhou Medical University ⁴ Key Laboratory of Systems Biomedicine (Ministry of Education), Shanghai Center for Systems Biomedicine, Shanghai Jiao Tong University ⁵ Department of Physics and Astronomy, University of California, Irvine ⁶ Department of Chemistry, University of California, Irvine ⁷ NSF-Simons Center for Multiscale Cell Fate Research, University of California, Irvine

*These authors contributed equally

Corresponding Author

Jin Yu

jin.yu@uci.edu

Citation

E, C., Dai, L., Tian, J., Da, L.T., Yu, J. Structure-Based Simulation and Sampling of Transcription Factor Protein Movements along DNA from Atomic-Scale Stepping to Coarse-Grained Diffusion. *J. Vis. Exp.* (181), e63406, doi:10.3791/63406 (2022).

Date Published

March 1, 2022

DOI

10.3791/63406

URL

jove.com/video/63406

Introduction

Transcription factors (TF) search for the target DNA to bind and regulate gene transcription and related activities¹. Aside from the three-dimensional (3D) diffusion, the facilitated diffusion of TF has been suggested to be essential for target

DNA search, in which the proteins can also slide or hop along one-dimensional (1D) DNA, or jump with intersegmental transfer on the DNA^{2,3,4,5,6,7}.

Abstract

One-dimensional (1-D) sliding of transcription factor (TF) protein along DNA is essential for facilitated diffusion of the TF to locate target DNA site for genetic regulation. Detecting base-pair (bp) resolution of the TF sliding or stepping on the DNA is still experimentally challenging. We have recently performed all-atom molecular dynamics (MD) simulations capturing spontaneous 1-bp stepping of a small WRKY domain TF protein along DNA. Based on the 10 μ s WRKY stepping path obtained from such simulations, the protocol here shows how to conduct more extensive conformational samplings of the TF-DNA systems, by constructing the Markov state model (MSM) for the 1-bp protein stepping, with various numbers of micro- and macro-states tested for the MSM construction. In order to examine processive 1-D diffusional search of the TF protein along DNA with structural basis, the protocol further shows how to conduct coarse-grained (CG) MD simulations to sample long-time scale dynamics of the system. Such CG modeling and simulations are particularly useful to reveal the protein-DNA electrostatic impacts on the processive diffusional motions of the TF protein above tens of microseconds, in comparison with sub-microseconds to microseconds protein stepping motions revealed from the all-atom simulations.

In a recent study, we have conducted tens of microseconds (μ s) all-atom equilibrium molecular dynamics (MD) simulations on a plant TF - the WRKY domain protein on the DNA⁸. A complete 1-bp stepping of WRKY on poly-A DNA within microseconds has been captured. The movements of the protein along the DNA groove and hydrogen bonds (HBs) breaking-reforming dynamics have been observed. While such a trajectory represents one sampled path, an overall protein stepping landscape is still lack of. Here, we show how to expand computational samplings around the initially captured protein stepping path with the constructed Markov state model (MSM), which have been implemented widely for simulating a variety of biomolecular systems involving substantial conformational changes and time-scale separation^{9, 10, 11, 12, 13, 14, 15, 16, 17, 18, 19}. The purpose is to reveal the conformational ensemble and meta-stable states of the TF protein diffusion along DNA for one cyclic step.

While the above MD simulation reveals atomic resolution of the protein movements for 1 bp on the DNA, the structural dynamics of long-time processive diffusion of the TF along DNA at the same high-resolution is hardly accessible. Conducting coarse-grained (CG) MD simulations at residue level is however technically approachable. The CG simulation time scale can be effectively extended to tens or hundreds of times longer than the atomic simulations^{20, 21, 22, 23, 24, 25, 26, 27, 28, 29}. Here, we show the CG simulations conducted by implementing the CafeMol software developed by Takada lab³⁰.

In current protocol, we present the atomic simulations of the WRKY domain protein along poly-A DNA and the MSM construction first, which focus on sampling the protein stepping motions for only 1 bp along DNA. Then we present the CG modeling and simulations of the same protein-DNA

system, which extend the computational sampling to the protein processive diffusion over tens of bps along DNA.

Here, we use GROMACS^{31, 32, 33} software to conduct MD simulations and MSMbuilder³⁴ to construct the MSM for sampled conformational snapshots, as well as to use VMD³⁵ to visualize the biomolecules. The protocol requires that the user to be able to install and implement the software above. The installation and implementation of the CafeMol³⁰ software is then necessary for conducting the CG MD simulations. Further analyses of the trajectories and visualization are also conducted in VMD.

Protocol

1. Construction of the Markov state model (MSM) from atomic MD simulations

1. Spontaneous protein stepping pathway and initial structures collection
 1. Use a previously obtained 10- μ s all-atom MD trajectory⁸ to extract 10000 frames evenly from a "forward" 1-bp stepping path (i.e., one frame for each nanosecond). The total number of frames needs to be sufficiently large to include all representative conformations.
 2. Prepare the transition path with 10000 frames in VMD by clicking **File > Save coordinates**, type protein or nucleic in selected atoms box and choose frames in Frames box, click **Save** to get the frames needed.

NOTE: A previously obtained 10 μ s all-atom MD simulation trajectory (called "forward stepping trajectory" here) for WRKY stepping 1-bp distance on a 34-bp homogeneous poly-A DNA⁸ was used

as the initial path to launch further conformational samplings. Note that in most of practices, however, an initial path is constructed, by performing steered or targeted MD simulations, or implementing general path-generation methods, etc.^{36,37,38,39}.

- Align the long axis of the reference DNA (from crystal structure) to the x-axis, and set the initial center of mass (COM) of the full 34-bp DNA at the origin of the coordinate space for the convenience of further data analysis. To do this, click **Extensions > Tk Console** in VMD, and type in the Tk console command window:

```
source rotate.tcl
```

The tcl script can be found in **Supplementary File 3**.

- Then calculate the root-mean-square-distance (RMSD) of the protein backbone by aligning the central 10 bp DNA (A 14 to 23 and T 14' to 23') to that from the crystal structure⁴⁰, and the RMSD represent geometrical measures of the systems (see **Figure 1A**). Do this by clicking **VMD > Extensions > Analysis > RMSD trajectory tool** and type nucleic and residue 14 to 23 and 46 to 55 in atom selection box, click **Align** and then **RMSD** box to calculate the RMSD values.
- Calculate the rotational degree of protein around DNA $\Theta(t)$ on the y-z plane in MATLAB by typing the command

```
rad2deg(atan(z/y))
```

with the initial angular positioning defined as $\Theta(0)=0$, as conducted previously⁸.
- Type the following command in MATLAB⁴¹ to use K-means methods^{42,43,44} and classify the 10000 structures into 25 clusters by typing:

```
[idx, C]=kmeans( X, 25)
```

here X is a 2D matrix of RMSD and rotational angle of WRKY on the DNA. Gather the structures of these 25 cluster centers for further MD simulations.

NOTE: Since the protein RMSD sampled relative to DNA covers a range of about 25 Å, we choose 25 clusters to have one cluster per angstrom.

- Conducting the 1st round of MD simulations and the simulation settings
 - Build atomistic systems for the 25 structures by using GROMACS 5.1.2 software³² under parmbsc1 force field⁴⁵ and by using the buildsystem.sh file from **Supplementary File 2** in shell.
 - Conduct 60-ns MD simulations for these 25 systems under NPT ensemble with a time step of 2 fs by typing the following command in shell:

```
gmx_mpi grompp -f md.mdp -c npt.gro -p topol.top -o md.tpr
```

```
gmx_mpi mdrun -deffnm md
```
- Clustering the 1st round MD trajectories
 - Remove the first 10 ns of each simulation trajectory by typing in shell:

```
gmx_mpi trjcat -f md.xtc -b 10000 -e 600000 -o newtraj.xtc
```

and collect conformations from the 25 × 50 ns trajectories for clustering to prepare the input structures for the subsequent more extensive samplings (2nd round MD simulations).
NOTE: To reduce the impact from the initial path and to allow local equilibration, 10-ns of the initial period of simulations were removed.

- Choose distance pairs between protein and DNA as input parameters for the time-independent component analysis (tICA)^{46,47,48} projection. Use the `make_ndx` command in GROMACS to do that:

```
gmx_mpi make_ndx -f input.pdb -o index.ndx
```

NOTE: Here, the protein CA atoms and the heavy atoms (NH1, NH2, OH, NZ, NE2, ND2) of residue Y119, K122, K125, R131, Y133, Q146, K144, R135, W116, R117, Y134, K118, Q121 that can form hydrogen bonds (HBs) with the DNA nucleotide were selected, which pair with the O1P O2P and N6 atoms of the DNA nucleotide (A14-20, T19-23). The selected amino acids can either form stable HBs or salt bridges with DNA.

- Copy the above selected atom index from `index.ndx` file to a new text file (`index.dat`). Get the pair information between these atoms by the python script from **Supplementary File 1** `generate_atom_indices.py` and type:

```
python2.6 generate_atom_indices.py index.dat > AtomIndices.txt
```

This generates the 415 distance pairs between protein and DNA.

- Calculate the 415 distance pairs from every trajectory by typing the following command in MSMbuilder command window:

```
mshmb AtomPairsFeaturizer -out pair_features --pair_indices AtomIndices.txt --top references.pdb --trjs "trajectories/*.xtc" --transformed pair_features --stride 5
```

- Conduct tICA to reduce the dimension of data onto the first 2 time-independent components (tICs) or vectors by typing:

```
mshmb tICA -i ./tica_rc_a/tmp/ -o tica_results --n_components 2 --lag_time 10 --gamma 0.05 -t tica_results.h5
```

NOTE: tICA is a dimension-reduction method that calculates the eigenvalue of time-lagged correlation matrix $C_{ij}^{(\Delta t)}$ to determine the slowest relaxing degrees of freedom of the simulation system by the equation:

$$C_{ij}^{(\Delta t)} = \mathbb{E}^n[X_i(t)X_j(t + \Delta t)]$$

where $X_i(t)$ is the value of the i -th reaction coordinate at time t , and $X_j(t+\Delta t)$ is the value of the j -th reaction coordinate at time $t+\Delta t$. \mathbb{E} is the expectation value of the product of the $X_i(t)$ and $X_j(t + \Delta t)$ overall simulation trajectories. The directions along the slowest relaxing degrees of freedom correspond to the largest eigenvalues of the above time-lagged

correlation matrix $C_{ij}^{(\Delta t)}$. Here, 2 tICs seem to be a minimal set to differentiate three macrostates upon our MSM construction (addressed later). One can also calculate the generalized matrix Rayleigh quotient (GMRQ) score⁴⁹, for example, to explore an optimal set of components to be used.

- Use command in MSMbuilder to cluster the projected datasets into 100 clusters by K-center^{43,44} method (see **Figure 1B**):

```
mshmb KCenters -i ./tica_results.h5 -o kcenters_output -t kcenters_output --n_clusters 100.
```

Select the center structure of each cluster as the initial structure for the 2nd round of MD simulations. Maintain the simulation information of the simulated 100 structures, including positions, temperatures, pressures, etc., except for the velocities.

NOTE: After the first round of 25 simulations, the memory of the initial path has been reduced, so we generate more clusters, e.g., 100 clusters, in the second round, to substantially expand the conformational samplings.

4. Conducting the 2nd round extensive MD simulations

1. Conduct 60-ns MD simulations starting from these 100 initial structures after imposing random initial velocities on all the atoms. Add the random initial velocities by turning on the velocity generation in mdp file, i.e., changing the md.mdp file `gen_vel = no` to `gen_vel = yes`.
2. Remove the first 10 ns of each simulation as described in step 1.3.1, collect 2,500,000 snapshots from the 100 × 50 ns trajectories evenly to construct the MSM.

NOTE: Note that in the later macrostates construction, a small number of off-path states with a particularly low population (~0.2%, on the bottom of X-Θ plane) were found. These off-path states are classified as one macrostate when the total number of macrostates is set as 3 to 6 (**Figure 2B**). Since such a low population macrostate includes only 3 trajectories, which were removed in the end, the results shown in this protocol were obtained indeed from 97 × 50 ns trajectories, with a total of 2,425,000 frames or snapshots.

5. Clustering the 2nd round MD trajectories

1. Conduct tICA for the 2nd round trajectories as done previously. Type in MSMbuilder:

```
msmb tICA -i ../tica_rc_a/tmp/ -o tica_results --n_components 2 --lag_time 10 --gamma 0.05 -t tica_results.h5
```

2. Calculate the implied timescale to validate parameters for the correlation delay time Δt and microstates numbers (see **Figure 1C**),

$$\tau_k = -\tau / \ln \mu_k(\tau),$$

where τ represents the lag-time used for building the transition probability matrix (TPM); $\mu_k(\tau)$ represents the k th eigenvalue of the TPM under a lag time of τ . Use the python script from **Supplementary File 1** for this python `BuildMSMsAsVaryLagTime.py -d ../ -f ../trajlist_num -i 50 -m 1000 -t 10 -n 20 -s 500`.

3. Vary the lag-time τ and microstates number by changing the parameters used above:

```
python BuildMSMsAsVaryLagTime.py -d ../ -f ../trajlist_num -i 50 -m 1000 -t 5 10 20 30 40 -n 20 -s 20 200 400 500 800 2000
```

NOTE: The system is regarded as Markovian when the implied timescale curves start to level off with time-scale separation. Then, choose the Δt as the correlation delay time, and the τ the lag time where the implied timescale starts to level off to build MSM.

4. Accordingly, choose a comparatively large (but not too large) number of states, $N = 500$, and a comparatively short correlation delay time $\Delta t = 10$ ns. The lag time was found to be $\tau = 10$ ns to build MSM.
5. Classify the conformations into 500 clusters (see **Figure 1D**) by using the command:

```
msmb KCenters -i ../tica_results.h5 -o kcenters_output -t kcenters_output --n_clusters 500
```

6. MSM construction

1. Lump the 500 microstates into 3–6 macrostates to find out the number of macrostates which suit best according to the PCCA+ algorithm⁵⁰ in MSMbuilder, by using the python script in **Supplementary File**

1 python msm_lumping_usingPCCAplus.py. Identify a reduced kinetic network of models for the most essential conformational changes of biomolecules, by constructing a small number of macrostates, i.e., upon kinetically lumping hundreds of microstates as described below^{17,51}.

2. Map the high-dimensional conformations to the X (protein movement along the DNA long axis) and rotational angle of the protein along the DNA for each macrostate as described in step 1.1.3 and 1.1.4 (e.g., no state with too low population < 1%; see **Figure 2C**). Then find the 3 macrostates that best represent the system (**Figure 1E**). See **Figure 2D** for snapshots of the movement of protein along DNA and the protein rotation angle around DNA.

NOTE: In previous work generating the 10 μ s spontaneous protein forward stepping path, we additionally conducted 5 x 4 μ s equilibrium MD simulations to moderately expand the samplings. We showed the mapping of the original forward path (see **Figure 2A** left) and further 4- μ s sampling trajectories on the forward path conducted previously (see **Figure 2A** right)⁸. The mapping of the original 100 x 50 ns (see **Figure 2B** left)⁸ and the 97 x 50 ns trajectories used in this work are shown (see **Figure 2B** right).

7. Calculation of the mean first passage times (MFPT)
 1. Conduct five 10-ms Monte Carlo (MC) trajectories based on the TPM of the 500 microstate MSM with the lag time of 10 ns set as the time step of MC. Calculate MFPT⁵² between each pair of macrostates (**Figure 3**) by the python

script in **Supplementary File 1** python python mfpt_msm3.py.

2. Calculate the average and standard error of the MFPT using the bash file in **Supplementary File 2**, type:

```
sh mfpt_analysis.bash
```

2. Conducting coarse-grained (CG) simulation to sample long-time dynamics

1. Conduct a CG simulations by using the CafeMol 3.0 software³⁰. See the CG simulation settings specified in the input configuration file with an extension .inp, including input structures, simulation parameters, output files, etc. Type the following command on the terminal to run the CG simulation:

```
cafemol XXX.inp
```

2. Specify the following blocks in the input file, with each block starting with the label <<<< and ending with >>>>.

1. Set filenames block (required) to specify the working directories and input/output file store path. Type following for the filenames block for these simulations:

```
<<<< filenames
path = XXXXX (working path)
filename = wrky (the output file names)
OUTPUT psf pdb movie dcd rst
path_pdb = XXXXX (input native structure path)
path_ini = XXXXX (input initial structure path)
path_natinfo = XXXXX (native information file path)
path_para = XXXXX (parameter files path)
>>>>
```

NOTE: As the Go-model⁵³ is utilized in the CG modeling, i.e., protein will be biased to the native conformation, so one needs to set the modeled

structure as the native conformation. Here, the input crystal structure was set as the native conformation.

2. Set the job control block (required) to define the running mode of the simulations. Type the following command:

```
<<<< job_ctl
i_run_mode = 2 (= 2 the constant temperature
simulation)
i_simulate_type = 1 (=1 Langevin dynamics)
i_initial_state = 2 (=2 means the initial configuration
is Native configuration)
>>>>
```

Select the constant temperature Langevin dynamics simulations.

3. Set the unit and state block (required) to define the information for input structures. Type the following command:

```
<<<< unit_and_state
i_seq_read_style = 1 (=1 means read sequences
from PDB file)
i_go_native_read_style = 1 (=1 means the native
structure is from PDB file)
1 protein protein.pdb (unit&state molecular_type
native_structure)
2-3 dna DNA.pdb (unit&state molecular_type
native_structure)
>>>>
```

NOTE: The initial input structure files (protein.pdb and DNA.pdb here) are needed. The structures are written in the pdb format. Two pdb files are needed here: one is the protein structure file containing the heavy atom coordinates of WRKY (unit 1), and the other is the coordinates of 200-bp double-stranded

(ds) DNA (unit 2-3). The protein is initially placed 15 Å away from the DNA.

4. Set the energy function block (required) defined in the energy_function block. Type the following command:

```
<<<< energy_function
LOCAL(1) L_GO
LOCAL(2-3) L_DNA2
NLOCAL(1/1) GO EXV ELE
NLOCAL(2-3/2-3) ELE DNA
NLOCAL(1/2-3) EXV ELE
i_use_atom_protein = 0
i_use_atom_dna = 0
i_para_from_ninfo = 1
i_triple_angle_term = 2
>>>>
```

NOTE: In the CG simulations, the protein is coarse-grained by the Go-model⁵³ with each amino acid represented by a CG particle placed at its C α position. The protein conformation will be biased then towards the native structure, or crystal structure here, under the Go potential (**Figure 4A** left). The DNA is described by the 3SPN.2 model⁵⁴, in which each nucleotide is represented by 3 CG particle S, P, N, which correspond to sugar, phosphate, and nitrogenous base, respectively (**Figure 4A** right). The electrostatic and vdW interactions are considered between different chains. The electrostatic interactions between protein and DNA in the CG simulation are approximated by the Debye-Hückel potential⁵⁵. The vdW repulsive energy takes the same form as in the Go model.

- Set the `md_information` block (required) to define the simulation information. Type the following command:

```
<<<< md_information
n_step_sim = 1
n_tstep(1) = 50000000
tstep_size = 0.1
n_step_save = 1000
n_step_neighbor = 100
i_com_zeroing = 0
i_no_trans_rot = 0
tempk = 300.0
n_seed = -1
>>>>
```

The `n_tstep` is the simulation step. Set the `tstep_size` as the time length of each MD step, each CG Cafemol time step is about 200 fs³⁰, so each MD step here is 200 × 0.1 fs in principle. Update the neighbor list every 100 MD steps (`n_step_neighbor = 100`). Set the simulation temperature to 300 K. Control the temperature by employing the velocity-type Verlet algorithm for updating protein structure with the Berendsen thermostat⁵⁶.

NOTE: The `n_step_sim` is the basin number of the Go model based potential, or the local minimal number of the energy curve. A multiple-basin potential allows the protein conformation biased to different conformations so that protein conformation can change from one local minimum to another. Here only the single basin Go model is used, which means only one biased conformation (crystal structure) for protein in the simulations. Meanwhile, since there is no protein-DNA hydrogen bonding interaction, etc. modeled in the CG context, the

molecular motions can be sampled even faster, i.e., > 10 times than in the atomic simulations.

- Set electrostatic block (required only when electrostatic interaction is used) as the electrostatic interaction is considered among different chains, so use this block to the define the parameters for electrostatic interaction by typing:

```
<<<< electrostatic
cutoff_ele = 10.0
ionic_strength = 0.15
>>>>
```

Set the Debye length in the electrostatic interaction to 10 Å, corresponding to the solution condition. Set the ionic strength to 0.15 M, as at the physiological condition.

Representative Results

Rotation-coupled sliding or 1 bp stepping of WRKY from the MSM construction

All protein conformations on the DNA are mapped to the longitudinal movement X and rotation angle of the protein COM along DNA (see **Figure 3A**). The linear coupling of these two degrees indicates rotation-coupled stepping of the WRKY domain protein on the DNA. The conformations can be further clustered into 3 macrostates (S1, S2, and S3) in the MSM. The forward stepping of WRKY then follows the macrostate transition S1->S2->S3. S1 refers to a metastable state initiated by the modeled structure (based on the crystal structure of WRKY-DNA complex⁴⁰), with a population of ~ 6%. Note that in current modeling, the initial protein conformation was adopted from the crystal structure in which the protein binds with specific W-box DNA sequence⁴⁰. Such a modeled protein-poly A-DNA complex thus leads to less favorable initial structures (S1) than the stepped or finally

relaxed structures (S3). Nevertheless, one can find that the hydrogen bonds (HBs) at the protein-DNA interface recover near the center of S3 as that near the center in S1 (see **Figure 3B**). The HBs in the S1 state are well maintained: K125 with A15, R131, Q146 and Y133 with A16, K144 and Y119 with A17, R135 with A18 (**Figure 3B** top left). S3 refers to a metastable state after the 1-bp protein stepping, with almost all the HBs shifted for 1-bp distance (**Figure 3B** bottom), and the structures appear stable with the highest population (63%). The intermediate state S2 connects S1 and S3, with a medium-high population (~30%). We found that the R135 and K144 are quite flexible in this intermediate state and can usually break HBs with the current nucleotide and reform that with the next nucleotide (**Figure 3B** top right). Overall, the WRKY protein COM moved ~2.9 Å and rotated ~55° to stepping 1 bp here. The rate-limiting step for the WRKY stepping is S2->S3, which essentially allows collective breaking and reforming of the HBs and requires ~7 μs on average. In contrast, S1 to S2 can transit very fast at a time of ~0.06 μs or 60-ns (**Figure 3B**), involving mainly the protein COM fluctuations (e.g., due to protein orientational changes on the DNA).

Single-strand bias of WRKY during processive diffusion in the CG model

In our recent study, we found that the WRKY domain protein binds preferentially to one strand of the dsDNA, no matter during 1-bp stepping or static binding; and the single-strand bias becomes highly prominent particularly upon specific DNA sequence binding⁸. Meanwhile, it is not clear whether such a trend remains during the processive diffusion of the protein along DNA. Here we tried to examine the potential strand bias *via* the CG simulations. Interestingly, a significant single-strand DNA binding configuration has been identified in the CG simulations of the WRKY during processive diffusion.

To see that, the contact numbers between protein and DNA were calculated on the respective DNA strands (see **Figure 4B**). A contact is considered when the distance between protein CG particle and DNA CG P (phosphate group) particle is smaller than 7 Å. The protein indeed shows bias to one of the DNA strands (e.g., ~4 contacts to one strand and ~1 contact to the other), i.e., even when detailed interactions such as HBs at the protein-DNA interface are not modeled.

The preferred DNA strand, however, can switch from time to time between the two strands of the DNA, depending on the binding orientation or configuration of the protein on the DNA. In particular, according to the contact number formed between the protein and respective strands of DNA, there are mainly 4 states here (as labeled 1, 2, 3, and 4 in **Figure 4B,C**). In state 1 and 3, a zinc-finger region binds toward -Y direction, and the preferred strand is the blue one. In state 2 and 3, the zinc-finger region binds toward +Y direction, and the preferred strand becomes the red one. It is also found that the zinc-finger region interacts dominantly with the DNA (see **Figure 4D**). Hence, the DNA strand bound closely with the zinc-finger region is indeed the preferred one. According to the above sampling, it thus appears that the strand bias persists but switches between the two DNA strands in the CG model of the processive protein diffusion.

Protein individual residual stepping in the CG simulations

It was previously noticed from our CG simulations that the stepping size of WRKY may vary on different DNA sequences⁸. The protein COM tends to step 1 bp on the homogeneous poly-A DNA. While on poly-AT DNA with 2 bp periodicity, the proportion of 2-bp stepping seems to increase.

Additionally, here we examined whether individual protein residues move synchronously at the protein-DNA interface.

We calculated the stepping size of each highly conserved residue in the WRKY motif (WRKYGQK) for every 1000 timesteps (**Figure 5A**). The residual stepping size of each conserved residue can thus be measured from the CG

simulations. The results indeed show that the stepping sizes of these individual residues are more synchronized on poly-A DNA than on poly-AT or random DNA sequences (**Figure 5B**).

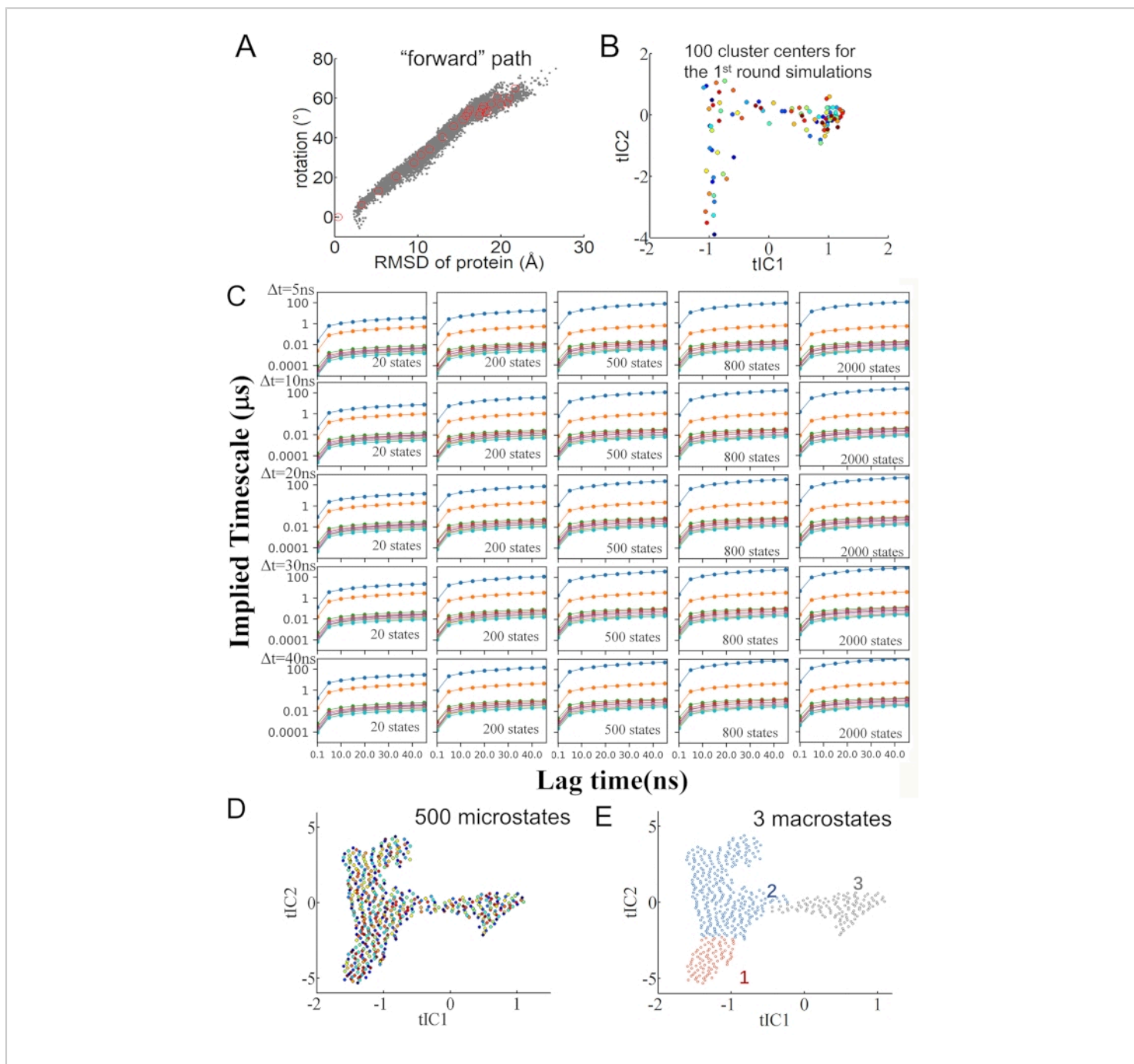


Figure 1: The conformations generation and microstates/macrostates construction. (A) The initial forward stepping path mapped on the protein-DNA RMSD and protein rotational angle around the DNA. The initial chosen 25 structures are

labeled by red circles. **(B)** The 100 conformation cluster centers from the 1st round 25 x 50 ns MD simulation trajectories mapped on the two highest eigenvalue tICs direction. **(C)** Plots of the implied timescale as a function of lag-time for the MSM construction *via* tICA using chosen distance pairs as input. For each set, MSM was constructed by projecting the conformations onto the top 2 tICs followed by K-centers clustering to produce 20 to 2000 microstates (from left to right column) with correlation delay time for tICA chosen from 5 to 40 ns (from top to bottom row). **(D)** The 500 microstates constructed and **(E)** the further constructed 3 macrostates, with corresponding microstate centers mapped along the highest two tICs direction. [Please click here to view a larger version of this figure.](#)

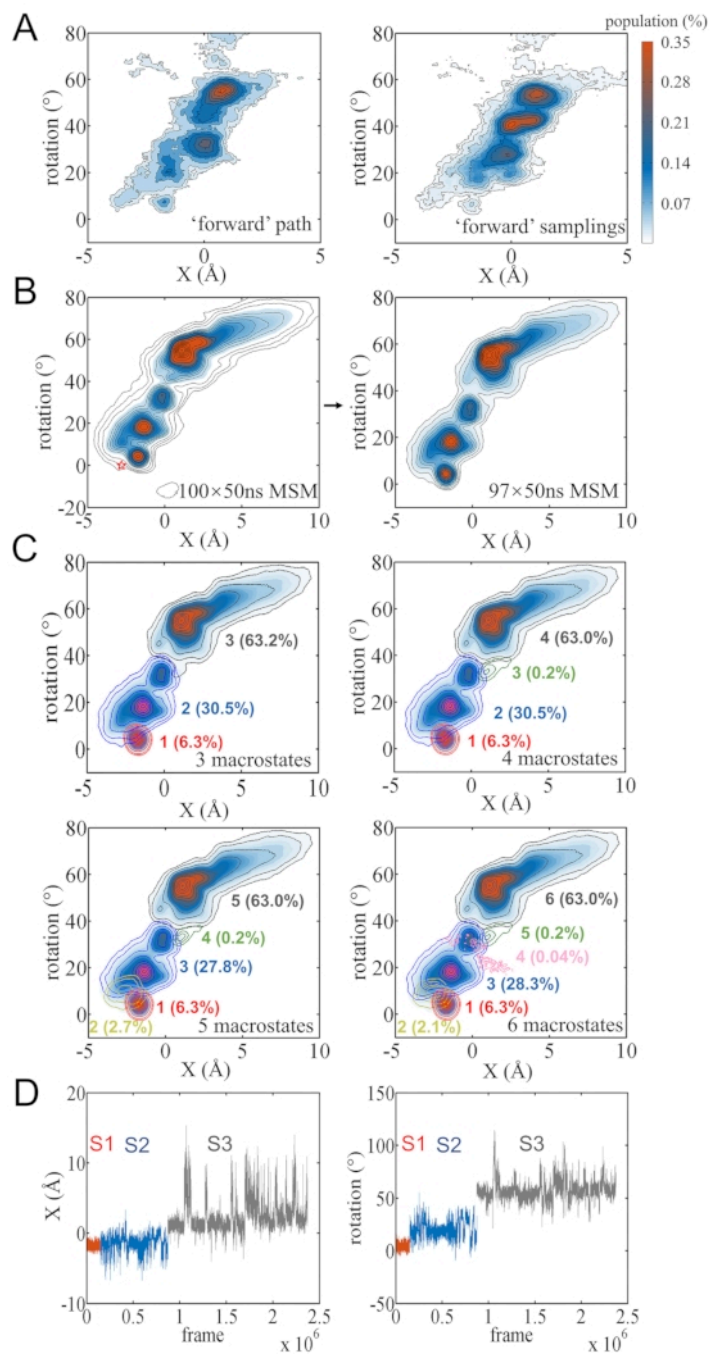


Figure 2: Construction of the macrostates. (A) The mapping of initial forward stepping path trajectory (left) and with a small number of additional micro-second trajectory samplings (right) on the protein center of mass (COM) movement along DNA long axis (X) and rotational angle around the DNA (obtained previously⁸). (B) The mapping of the original 100 × 50 ns trajectories and the 97 × 50 ns trajectories used in current MSM construction. (C) The construction of 3-6 macrostates and their populations from the constructed MSM are labeled on the extensive sampling maps. (D) The protein movement X and

rotation angle around DNA are shown, respectively. The sampled conformations are finally lumped into 3 macrostates, with red, blue, and gray corresponding to the macrostate 1, 2, and 3, respectively. [Please click here to view a larger version of this figure.](#)

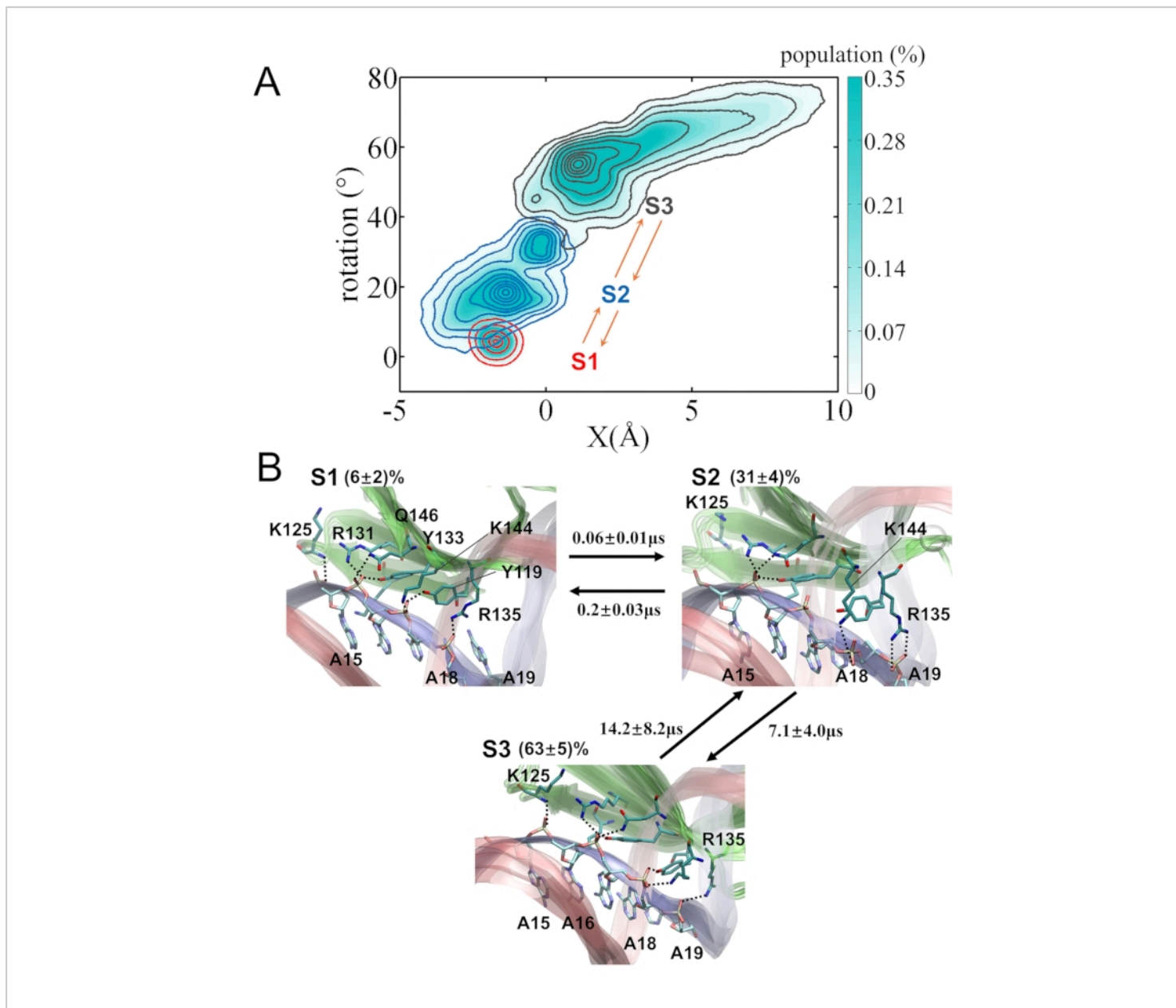


Figure 3: The MSM of the WRKY domain protein stepping on poly-A DNA. (A) The projection of the MD conformational snapshots onto coordinates of the protein COM movement X and rotational angle with respect to the DNA. The 3 macrostates S1, S2, and S3 are colored in red, blue, and gray, respectively. (B) Representative conformations and transition mean-first-passage-time (MFPT) of the constructed 3 macrostates. The key hydrogen bonds between protein and DNA are shown. [Please click here to view a larger version of this figure.](#)

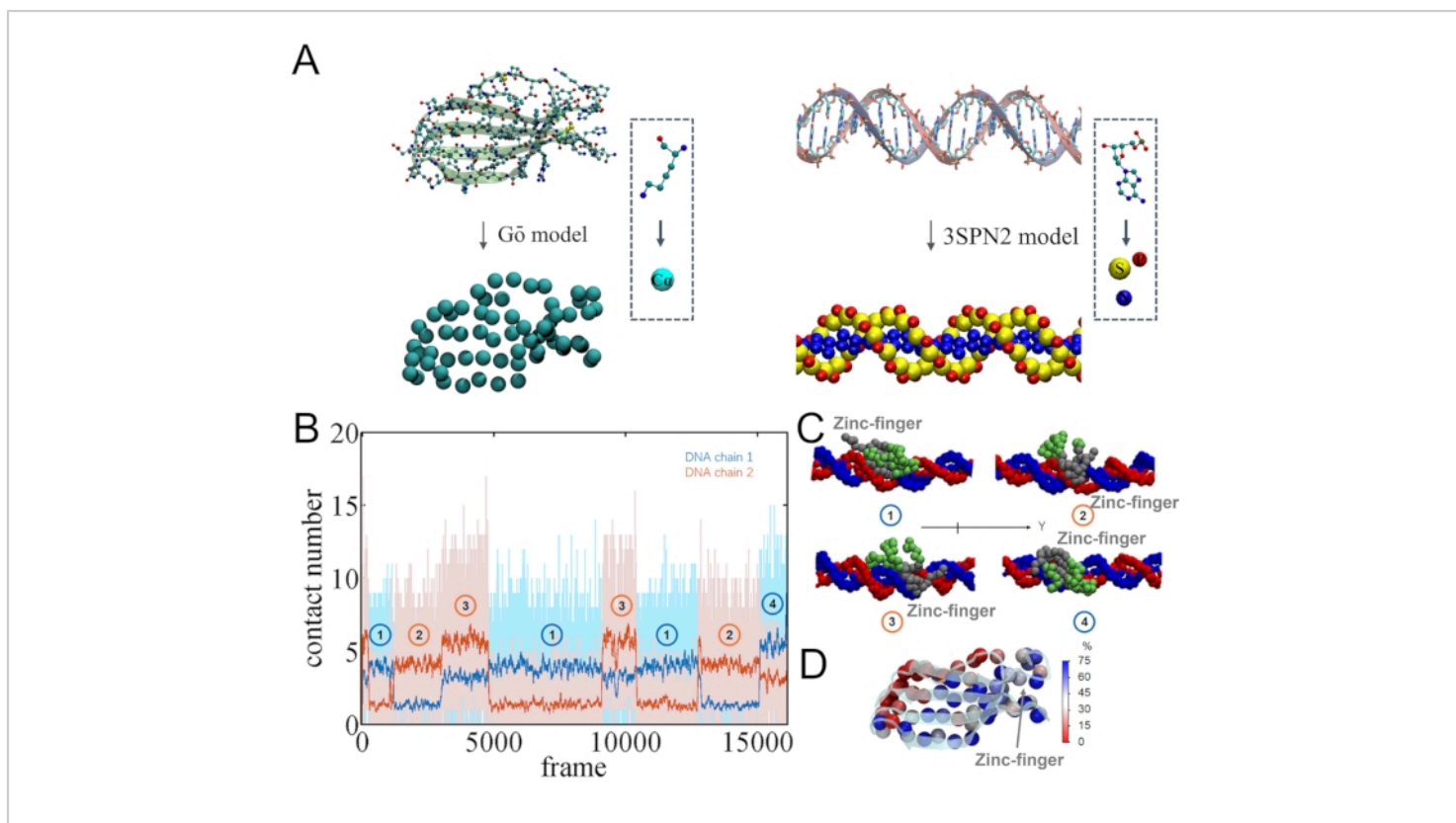


Figure 4: The coarse-grain (CG) model and contacts formed between protein and DNA strands in the CG model. (A) The coarse-graining of protein (left) and DNA (right). **(B)** The contact number between WRKY and each DNA strand along the simulation. **(C)** The molecular views of the 4 contact modes. The protein region near the zinc-finger is colored in gray, and the other region is colored in green. **(D)** The contact probability of each protein amino acid with DNA. When the distance between the CG particle of the amino acid and any DNA CG particles is smaller than 7 Å, the amino acid is considered to be in contact with DNA. [Please click here to view a larger version of this figure.](#)

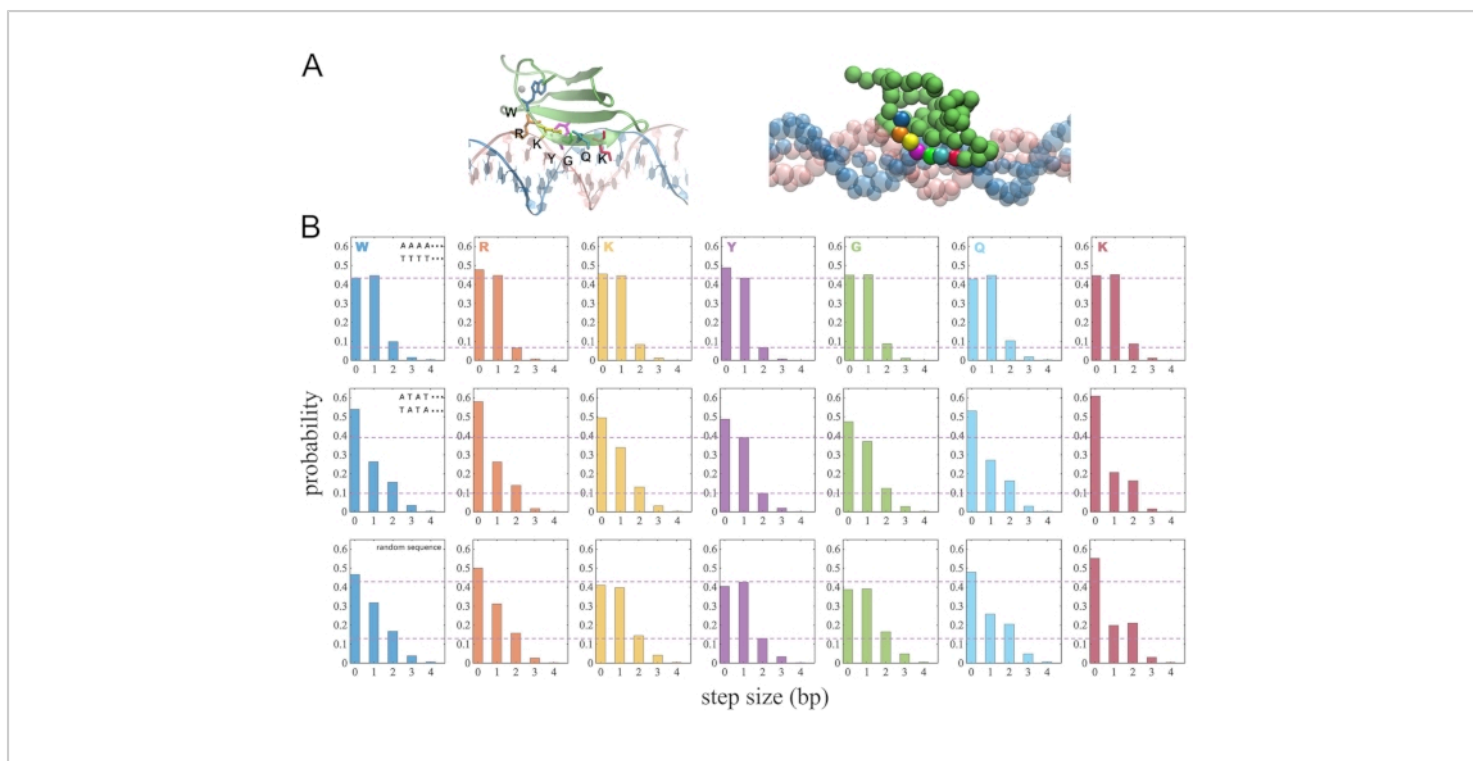


Figure 5: The diffusion step sizes of individual protein amino acid in the WRKY motif as WRKY moving along DNA. (A) The highly conserved residues (WRKYGQK) in atomic structure (left) and after coarse-graining (right). (B) The stepping size for each conserved residue on different sequences of DNA (poly-A; poly-AT; random sequences) [Please click here to view a larger version of this figure.](#)

Supplementary File 1: The python codes and software used in this protocol. MSM is built mainly by using the MSMbuilder, the necessary python codes are attached. [Please click here to download this File.](#)

Supplementary File 2: The atomistic molecular dynamics simulations are conducted by GROMACS, the commands and necessary files to build all-atom simulations are also attached. The coarse-grained simulations are conducted by CafeMol software. The simulation results are analyzed by VMD and MATLAB. [Please click here to download this File.](#)

Supplementary File 3: The tcl script to rotate and move protein in VMD. [Please click here to download this File.](#)

Discussion

This work addresses how to conduct structure-based computational simulation and samplings to reveal a transcription factor or TF protein moving along DNA, not only at atomic detail of stepping, but also in the processive diffusion, which is essential for the facilitated diffusion of TF in the DNA target search. To do that, the Markov state model or MSM of a small TF domain protein WRKY stepping for 1-bp along homogeneous poly-A DNA was first constructed, so that an ensemble of protein conformations on the DNA along with collective hydrogen bonding or HB dynamics at the protein-DNA interface can be revealed. To obtain the MSM, we conducted two rounds of extensive

all-atom MD simulations along a spontaneous protein stepping path (obtained from previous 10- μ s simulation), with current samplings in aggregation of 7.5 μ s (125 x 60 ns). Such extensive samplings provide us with snapshots for conformation clustering into hundreds of microstates, utilizing protein-DNA interfacial pair distances as geometric measures for the clustering. The Markovian property of the MSM construction is partially validated *via* detecting time-scale separation from the implied time scales calculated for various lengths or lag-time of individual MD simulations. 20–2000 microstates were then tested and compared for the time-scale separation properties, with 500 microstates selected for the MSM construction. Further, the 500 microstates were kinetically lumped into a small number of macrostates, for which we tested various number of states and found that three macrostates sufficient for the current system. The three-state model simply shows that state S1 transits to S2 comparatively fast (within tens of ns), dominated by protein center of mass (COM) fluctuations on the DNA, while state S2 transits to S3 slowly and is rate-limiting (\sim 7 μ s on average), dominated by collective HB dynamics for stepping. Note that kinetic lumping of the microstates into a small number of kinetically distinct macrostates is still subject to methodological developments, with different algorithms tested and machine learning techniques for improvements^{57, 58, 59, 60, 61, 62, 63}. The critical steps to build MSM include choosing the distance pairs used in tICA and determining the parameters used to construct microstates. The choice of distance pairs is knowledge based, and it is important to choose the most essential interaction pairs. The parameters for constructing microstates, such as the correlation delay time, lag time, the number of microstates, need to be properly set to ensure the system to be Markovian.

With such efforts, the submicro- to micro-seconds protein structural dynamics with atomic details can be systematically revealed for protein stepping 1-bp along DNA. In principle, with the transition probability matrix obtained from the MSM construction, the system can be evolved to a long time scale beyond microseconds, or say, to approach milliseconds and above^{13, 17, 64}. However, there are intrinsic limitations of the MSM sampling and construction, which rely on sub-microseconds individual simulations around a certain initial path, and the Markovian property may not be well guaranteed^{65, 66}. In most practices, the initial path was constructed under forcing or acceleration, though in the current system we take advantage of a spontaneous protein stepping path (without forcing or acceleration) obtained from a 10-ms equilibrium simulation⁸. The conformational samplings in aggregate are still limited by tens of microseconds due to high computational cost of the atomic simulations. Such microseconds samplings of the protein stepping are unlikely to provide sufficient conformations to appear on long-time scale processive TF diffusion. The memory issue would become significant if one implements the currently obtained transition probability matrix beyond a certain time scale, and the Markovian property is not guaranteed to ensure proper use of current MSM^{14, 52, 66}. Therefore, to sample the long-time scale processive diffusion of TF along DNA, the residue level coarse-grained or CG modeling and simulation are implemented instead, to balance between maintaining the structural basis and lowering the computational cost.

In the CG modeling and simulation, the protein residues and DNA nucleotides are represented by beads (i.e., one bead for one amino acid, and three beads for one nucleotide), with the protein conformation maintained *via* the Go model toward a native or pre-equilibrated configuration^{30, 53}. Though the atomic level of HB interactions becomes absent in the CG

model, the protein-DNA electrostatic interactions are well maintained, which seem to be able to capture dominant dynamics features in the processive diffusion of the protein along DNA^{67,68,69,70}. Detailed implementation protocols are presented for modeling and simulating the WRKY-DNA system here. The representative results show interestingly that first, the single-strand DNA bias presented in the previous atomic simulation of the WRKY-DNA system persists in the CG model, while a variety of protein orientations/configurations sampled during processive diffusion lead to switch of the bias between the two strands from time to time. Hence, such a DNA strand bias does not necessarily link to HB association but seems to rely mainly on the protein-DNA electrostatic interactions, which vary for various protein configurations or orientations on the DNA. Next, individual amino acids at or near the protein-DNA interface, such as the highly conserved WRKQGQK motifs, show different stepping sizes or synchronization patterns for different DNA sequences. In our previous study, the stepping size variations were shown only for the COM of protein, as the protein was modeled to diffuse along different DNA sequences. Note that the current CG model of the DNA supports DNA sequence variations with different parameterization^{54,71,72}, though atomic detail is missing. Proper DNA sequence-dependent parameterization in the structure-based modeling of the protein-DNA system, is thus critical to reveal protein-DNA search and recognition mechanisms across multiple time and length scales.

Disclosures

The authors have no conflict of interests.

Acknowledgments

This work has been supported by NSFC Grant #11775016 and #11635002. JY has been supported by the CMCF of UCI via NSF DMS 1763272 and the Simons Foundation grant #594598 and start-up fund from UCI. LTD has been supported by Natural Science Foundation of Shanghai #20ZR1425400 and #21JC1403100. We also acknowledge the computational support from the Beijing Computational Science Research Center (CSRC).

References

1. Latchman, D. S. Transcription factors: an overview. *The International Journal of Biochemistry & Cell Biology*. **29** (12), 1305-1312 (1997).
2. Berg, O. G., von Hippel, P. H. Selection of DNA binding sites by regulatory proteins. Statistical-mechanical theory and application to operators and promoters. *Journal of Molecular Biology*. **193** (4), 723-750 (1987).
3. von Hippel, P. H., Berg, O. G. Facilitated target location in biological systems. *The Journal of Biological Chemistry*. **264** (2), 675-678 (1989).
4. Halford, S. E., Marko, J. F. How do site-specific DNA-binding proteins find their targets? *Nucleic Acids Research*. **32** (10), 3040-3052 (2004).
5. Slusky, M., Mirny, L. A. Kinetics of protein-DNA interaction: facilitated target location in sequence-dependent potential. *Biophysical Journal*. **87** (6), 4021-4035 (2004).
6. Bauer, M., Metzler, R. Generalized facilitated diffusion model for DNA-binding proteins with search and recognition states. *Biophysical Journal*. **102** (10), 2321-2330 (2012).
7. Shvets, A. A., Kochugaeva, M. P., Kolomeisky, A. B. Mechanisms of Protein Search for Targets on DNA:

- Theoretical Insights. *Molecules (Basel, Switzerland)*. **23** (9), 2106 (2018).
8. Dai, L., Xu, Y., Du, Z., Su, X.D., Yu, J. Revealing atomic-scale molecular diffusion of a plant-transcription factor WRKY domain protein along DNA. *Proceedings of the National Academy of Sciences of the United States of America*. **118** (23), e2102621118 (2021).
 9. Chodera, J. D., Singhal, N., Pande, V. S., Dill, K. A., Swope, W. C. Automatic discovery of metastable states for the construction of Markov models of macromolecular conformational dynamics. *The Journal of Chemical Physics*. **126** (15), 155101 (2007).
 10. Pan, A. C., Roux, B. Building Markov state models along pathways to determine free energies and rates of transitions. *The Journal of Chemical Physics*. **129** (6), 064107 (2008).
 11. Bowman, G. R., Huang, X., Pande, V. S. Using generalized ensemble simulations and Markov state models to identify conformational states. *Methods (San Diego, California)*. **49** (2), 197-201 (2009).
 12. Prinz, J.H. et al. Markov models of molecular kinetics: Generation and validation. *The Journal of chemical physics*. **134** (17), 174105 (2011).
 13. Chodera, J. D., Noé, F. Markov state models of biomolecular conformational dynamics. *Current Opinion in Structural Biology*. **25**, 135-144 (2014).
 14. Malmstrom, R. D., Lee, C. T., Van Wart, A. T., Amaro, R. E. On the Application of Molecular-Dynamics Based Markov State Models to Functional Proteins. *Journal of Chemical Theory and Computation*. **10** (7), 2648-2657 (2014).
 15. Husic, B. E., Pande, V. S. Markov State Models: From an Art to a Science. *Journal of the American Chemical Society*. **140** (7), 2386-2396 (2018).
 16. Sittel, F., Stock, G. Perspective: Identification of collective variables and metastable states of protein dynamics. *The Journal of chemical physics*. **149** (15), 150901 (2018).
 17. Wang, W., Cao, S., Zhu, L., Huang, X. Constructing Markov State Models to elucidate the functional conformational changes of complex biomolecules. *WIREs Computational Molecular Science*. **8**, e1343 (2018).
 18. Peng, S. et al. Target search and recognition mechanisms of glycosylase AlkD revealed by scanning FRET-FCS and Markov state models. *Proceedings of the National Academy of Sciences of the United States of America*. **117** (36), 21889-21895 (2020).
 19. Tian, J., Wang, L., Da, L.T. Atomic resolution of short-range sliding dynamics of thymine DNA glycosylase along DNA minor-groove for lesion recognition. *Nucleic Acids Research*. **49** (3), 1278-1293 (2021).
 20. Chu, J.-W., Izveko, S., Voth, G. The multiscale challenge for biomolecular systems: coarse-grained modeling. *Molecular Simulation*. **32** (3-4), 211-218 (2006).
 21. Marrink, S. J., Risselada, H. J., Yefimov, S., Tieleman, D. P., De Vries, A. H. The MARTINI force field: coarse grained model for biomolecular simulations. *The Journal of Physical Chemistry B*. **111** (27), 7812-7824 (2007).
 22. Givaty, O., Levy, Y. Protein sliding along DNA: dynamics and structural characterization. *Journal of Molecular Biology*. **385** (4), 1087-1097 (2009).

23. Khazanov, N., Levy, Y. Sliding of p53 along DNA can be modulated by its oligomeric state and by cross-talks between its constituent domains. *Journal of Molecular Biology*. **408** (2), 335-355 (2011).
24. Riniker, S., Allison, J. R., van Gunsteren, W. F. On developing coarse-grained models for biomolecular simulation: a review. *Physical Chemistry Chemical Physics : PCCP*. **14** (36), 12423-12430 (2012).
25. Kmiecik, S. et al. Coarse-Grained Protein Models and Their Applications. *Chemical Reviews*. **116** (14), 7898-7936 (2006).
26. Bhattacharjee, A., Krepel, D., Levy, Y. Coarse-grained models for studying protein diffusion along DNA. *WIREs Computational Molecular Science*. **6**, 515-531 (2016).
27. Wang, J. et al. Machine Learning of Coarse-Grained Molecular Dynamics Force Fields. *ACS Central Science*. **5** (5), 755-767 (2019).
28. Joshi, S. Y., Deshmukh, S. A. A review of advancements in coarse-grained molecular dynamics simulations. *Molecular Simulation*. **47** (10-11), 786-803 (2021).
29. Bigman, L. S., Greenblatt, H. M., Levy, Y. What Are the Molecular Requirements for Protein Sliding along DNA? *The Journal of Physical Chemistry B*. **125** (12), 3119-3131 (2021).
30. Kenzaki, H. et al. CafeMol: A Coarse-Grained Biomolecular Simulator for Simulating Proteins at Work. *Journal of Chemical Theory and Computation*. **7** (6), 1979-1989 (2011).
31. Berendsen, H. J.C., van der Spoel, D., van Drunen, R. GROMACS: a message-passing parallel molecular dynamics implementation. *Computer Physics Communications*. **91** (1-3), 43-56 (1995).
32. van der Spoel, D. et al. GROMACS: fast, flexible, and free. *Journal of Computational Chemistry*. **26** (16), 1701-1718 (2005).
33. Abraham, M. J. et al. GROMACS: High performance molecular simulations through multi-level parallelism from laptops to supercomputers. *SoftwareX*. **1 - 2**, 19-25 (2015).
34. Harrigan, M. P. et al. MSMBuilder: Statistical Models for Biomolecular Dynamics. *Biophysical Journal*. **112** (1), 10-15 (2017).
35. Humphrey, W., Dalke, A., Schulten, K. VMD: visual molecular dynamics. *Journal of Molecular Graphics*. **14** (1), 33-38 (1996).
36. Izrailev, S. et al. Steered Molecular Dynamics. *In Computational Molecular Dynamics: Challenges, Methods, Ideas*. Springer, Berlin, Heidelberg. **4**, 39-65 (1999).
37. Schlitter, J., Engels, M., Krüger, P. Targeted molecular dynamics: a new approach for searching pathways of conformational transitions. *Journal of Molecular Graphics*. **12** (2), 84-89 (1994).
38. Maragliano, L., Fischer, A., Vanden-Eijnden, E., Ciccotti, G. String method in collective variables: minimum free energy paths and isocommittor surfaces. *The Journal of Chemical Physics*. **125** (2), 24106 (2006).
39. Weiss, D. R., Levitt, M. Can morphing methods predict intermediate structures? *Journal of Molecular Biology*. **385** (2), 665-674 (2009).
40. Xu, Y.P., Xu, H., Wang, B., Su, X.D. Crystal structures of N-terminal WRKY transcription factors and DNA complexes. *Protein & Cell*. **11** (3), 208-213 (2020).

41. Higham, D. J., Higham, N. J. *MATLAB guide*. Society for Industrial and Applied Mathematics (2016).
42. Hartigan, J. A., Wong, M. A. Algorithm AS 136: A K-Means Clustering Algorithm. *Journal of the Royal Statistical Society. Series C (Applied Statistics)*. **28** (1), 100-108 (1979).
43. Gonzalez, T. F. Clustering to minimize the maximum intercluster distance. *Theoretical Computer Science*. **38**, 293-306 (1985).
44. Zhao, Y., Sheong, F. K., Sun, J., Sander, P., Huang, X. A fast parallel clustering algorithm for molecular simulation trajectories. *Journal of Computational Chemistry*. **34** (2), 95-104 (2013).
45. Ivani, I. et al. Parmbsc1: a refined force field for DNA simulations. *Nature Methods*. **13** (1), 55-58 (2016).
46. Naritomi, Y., Fuchigami, S. Slow dynamics of a protein backbone in molecular dynamics simulation revealed by time-structure based independent component analysis. *The Journal of Chemical Physics*. **139** (21), 215102 (2013).
47. Naritomi, Y., Fuchigami, S. Slow dynamics in protein fluctuations revealed by time-structure based independent component analysis: the case of domain motions. *The Journal of Chemical Physics*. **134** (6), 065101 (2011).
48. Pérez-Hernández, G., Paul, F., Giorgino, T., De Fabritiis, G., Noé, F. Identification of slow molecular order parameters for Markov model construction. *The Journal of Chemical Physics*. **139** (1), 015102 (2013).
49. McGibbon, R. T., Pande, V. S. Variational cross-validation of slow dynamical modes in molecular kinetics. *The Journal of Chemical Physics*. **142** (12), 124105 (2015).
50. Deuffhard, P., Weber, M. Robust Perron cluster analysis in conformation dynamics. *Linear Algebra and its Applications*. **398**, 161-184 (2005).
51. Silva, D.A. et al. Millisecond dynamics of RNA polymerase II translocation at atomic resolution. *Proceedings of the National Academy of Sciences of the United States of America*. **111** (21), 7665-7670 (2014).
52. Swope, W. C., Pitner, J. W., Suits, F. Describing Protein Folding Kinetics by Molecular Dynamics Simulations. 1. Theory. *The Journal of Physical Chemistry B*. **108** (21), 6571-6581 (2004).
53. Clementi, C., Nymeyer, H., Onuchic, J. N. Topological and energetic factors: what determines the structural details of the transition state ensemble and "en-route" intermediates for protein folding? An investigation for small globular proteins. *Journal of molecular biology*. **298** (5), 937-953 (2000).
54. Hinckley, D. M., Freeman, G. S., Whitmer, J. K., De Pablo, J. J. An experimentally-informed coarse-grained 3-Site-Per-Nucleotide model of DNA: structure, thermodynamics, and dynamics of hybridization. *The Journal of chemical physics*. **139** (14), 144903 (2013).
55. Debye, P., Huckel, E. The theory of the electrolyte II- The border law for electrical conductivity. *Physikalische Zeitschrift*. **24**, 305-325 (1923).
56. Berendsen, H. J., Postma, J. V., van Gunsteren, W. F., DiNola, A., Haak, J. R. Molecular dynamics with coupling to an external bath. *The Journal of Chemical Physics*. **81**, 3684-3690 (1984).

57. Bowman, G. R. Improved coarse-graining of Markov state models via explicit consideration of statistical uncertainty. *The Journal of Chemical Physics*. **137** (13), 134111 (2012).
58. Jain, A., Stock, G. Identifying metastable states of folding proteins. *Journal of Chemical Theory and Computation*. **8** (10), 3810-3819 (2012).
59. Röblitz, S., Weber, M. Fuzzy spectral clustering by PCCA+: application to Markov state models and data classification. *Advances in Data Analysis and Classification*. **7**, 147-179 (2013).
60. Mardt, A., Pasquali, L., Wu, H., Noé, F. VAMPnets for deep learning of molecular kinetics. *Nature Communications*. **9** (1), 5 (2018).
61. Wang, W., Liang, T., Sheong, F. K., Fan, X., Huang, X. An efficient Bayesian kinetic lumping algorithm to identify metastable conformational states via Gibbs sampling. *The Journal of Chemical Physics*. **149** (7), 072337 (2018).
62. Chen, W., Sidky, H., Ferguson, A. L. Nonlinear discovery of slow molecular modes using state-free reversible VAMPnets. *The Journal of Chemical Physics*. **150** (21), 214114 (2019).
63. Gu, H. et al. RPnet: a reverse-projection-based neural network for coarse-graining metastable conformational states for protein dynamics. *Physical Chemistry Chemical Physics :PCCP*. **24** (3), 1462-1474 (2022).
64. Lane, T. J., Bowman, G. R., Beauchamp, K., Voelz, V. A., Pande, V. S. Markov state model reveals folding and functional dynamics in ultra-long MD trajectories. *Journal of the American Chemical Society*. **133** (45), 18413-18419 (2011).
65. Konovalov, K. A., Unarta, I. C., Cao, S., Goonetilleke, E. C., Huang, X. Markov State Models to Study the Functional Dynamics of Proteins in the Wake of Machine Learning. *JACS Au*. **1** (9), 1330-1341 (2021).
66. Cao, S., Montoya-Castillo, A., Wang, W., Markland, T. E., Huang, X. On the advantages of exploiting memory in Markov state models for biomolecular dynamics. *The Journal of Chemical Physics*. **153** (1), 014105 (2020).
67. Brandani, G. B., Takada, S. Chromatin remodelers couple inchworm motion with twist-defect formation to slide nucleosomal DNA. *PLoS Computational Biology*. **14** (11), e1006512 (2018).
68. Tan, C., Terakawa, T., Takada, S. Dynamic Coupling among Protein Binding, Sliding, and DNA Bending Revealed by Molecular Dynamics. *Journal of the American Chemical Society*. **138** (27), 8512-8522 (2016).
69. Terakawa, T., Takada, S. p53 dynamics upon response element recognition explored by molecular simulations. *Scientific reports*. **5**, 17107 (2015).
70. Brandani, G. B., Niina, T., Tan, C., Takada, S. DNA sliding in nucleosomes via twist defect propagation revealed by molecular simulations. *Nucleic Acids Research*. **46** (6), 2788-2801 (2018).
71. Knotts, T. A. 4th, Rathore, N., Schwartz, D. C., de Pablo, J. J. A coarse grain model for DNA. *The Journal of Chemical Physics*. **126** (8), 084901 (2007).
72. Freeman, G. S., Hinckley, D. M., Lequieu, J. P., Whitmer, J. K., de Pablo, J. J. Coarse-grained modeling of DNA curvature. *The Journal of Chemical Physics*. **141** (16), 165103 (2014).